Electronic Supplementary Information

Extracellular pH-driven targeted multifunctional manganese arsenite delivery system for tumor imaging and therapy

Ke Zhang,[a^] Hongyu Lin,[b^] Junjie Mao,[a^] Xiangjie Luo,[b] Ruixue Wei,[b] Zhongzhen Su,[a] Bin Zhou,[*a] Dan Li,[*a] Jinhao Gao,[*b] and Hong Shan[a]

[a] Center for Interventional Medicine, Guangdong Provincial Key Laboratory of Biomedical Imaging, and Guangdong Provincial Engineering Research Center of Molecular Imaging, The Fifth Affiliated Hospital, Sun Yat-sen University, Zhuhai, Guangdong 519000, China

[b] State Key Laboratory of Physical Chemistry of Solid Surfaces, The MOE Laboratory of Spectrochemical Analysis & Instrumentation, The Key Laboratory for Chemical Biology of Fujian Province, and Department of Chemical Biology, College of Chemistry and Chemical Engineering, Xiamen University, Xiamen 361005, China

[^] Equal contribution

*Email: jhgao@xmu.edu.cn; lidan25@mail.sysu.edu.cn; zhoub2@mail.sysu.edu.cn

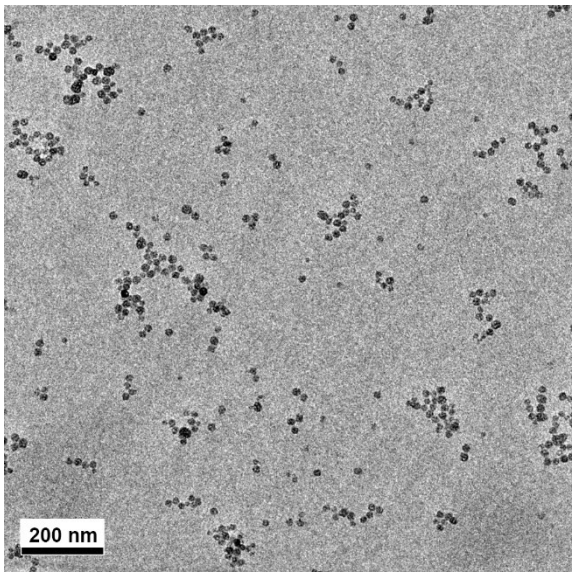

Figure S1. A representative TEM image of MnAs@SiO_2 NPs at low magnification.

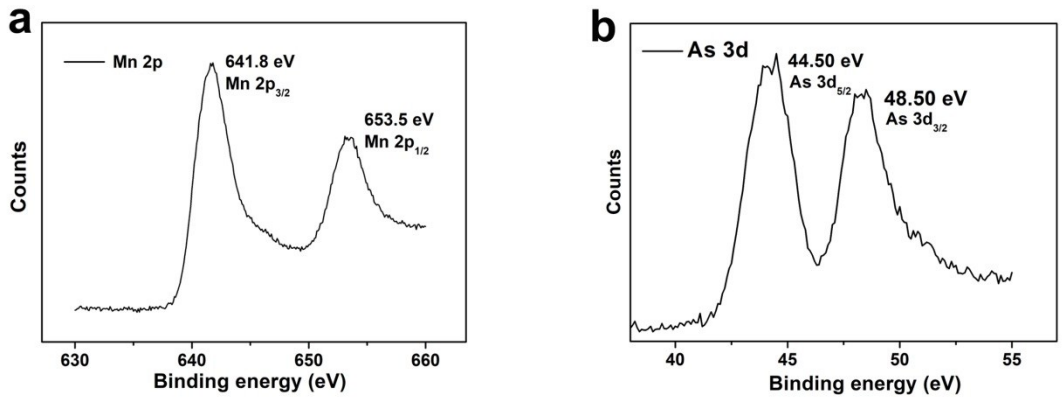

Figure S2. X-ray photoelectron spectroscopy (XPS) analysis of MnAs@SiO_2-pHLIP. (a) The peaks of Mn $2p_{3/2}$ and Mn $2p_{1/2}$ were at 641.8 eV and 653.5 eV, respectively. (b) The peaks of As $3d_{3/2}$ and $3d_{5/2}$ were at 44.50 eV and 48.50 eV, respectively.

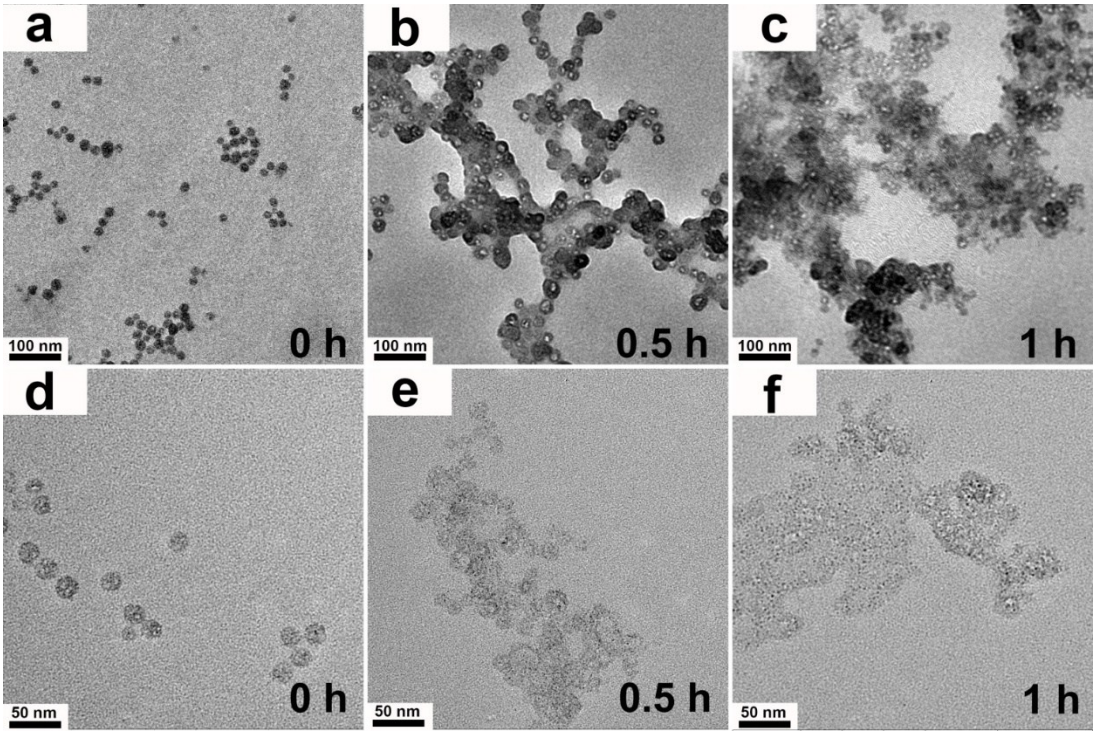

Figure S3. TEM images of MnAs@SiO_2 incubated in PBS buffer (pH = 6.0) for 0 h (a), 0.5 h (b), and 1 h (c). (d), (e), and (f) are corresponding TEM images at higher magnification.

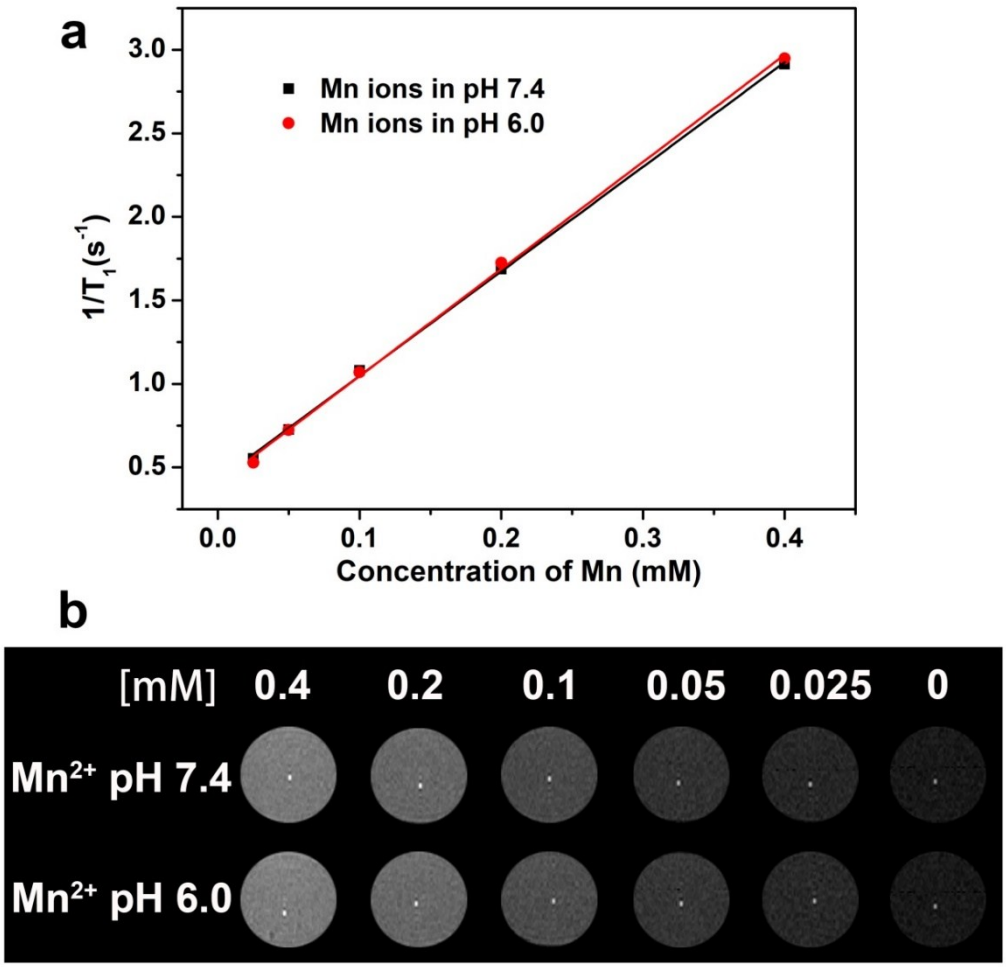

Figure S4. T_1-relaxivity measurements of Mn in pH 7.4 and pH 6.0 PBS buffer. (a) r_1 of $MnCl_2$ in different PBS buffers. (b) Phantom imaging of $MnCl_2$ in pH 7.4 and pH 6.0 buffers, respectively. All data were measured on a 0.5T NMI20-Analyst system.

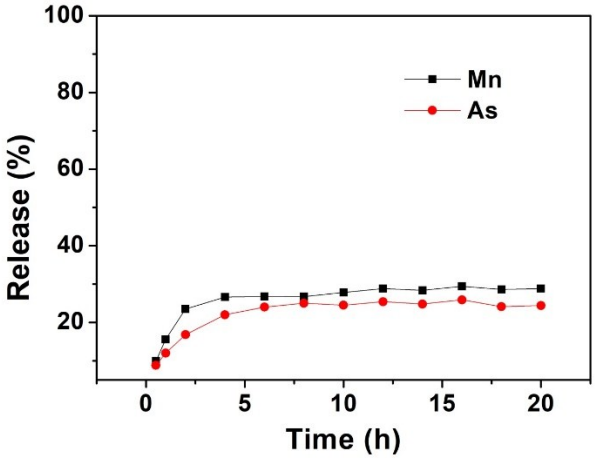

Figure S5. Quantitative drug release analysis of MnAs@SiO_2-pHLIP in blood serum. The concentration of Mn and As were measured by ICP-MS.

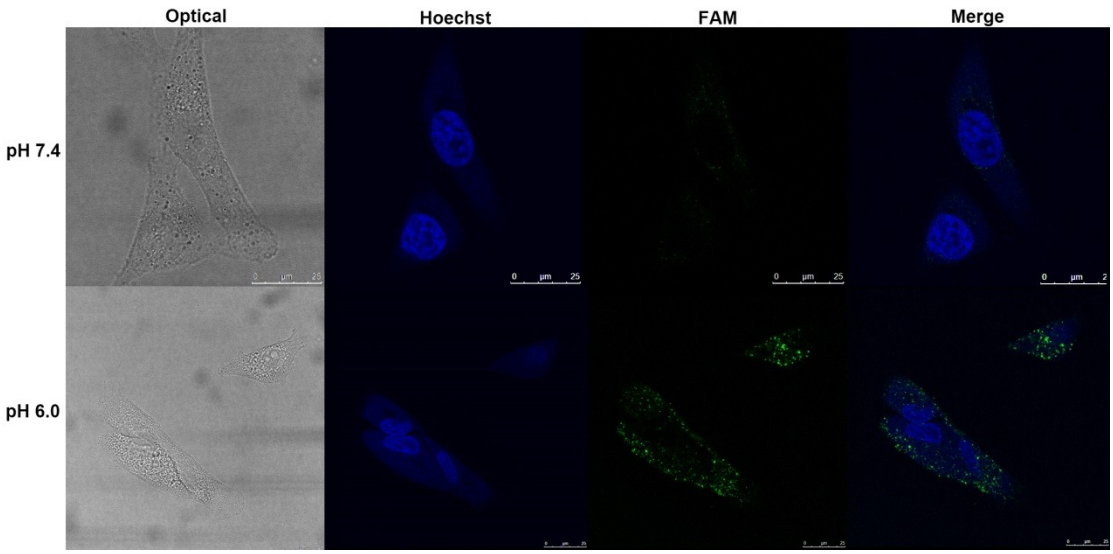

Figure S6. The targeted delivery ability of MnAs@SiO_2-pHLIP towards Hela cells. HeLa cells were incubated with MnAs@SiO_2-pHLIP for 2 h at pH 7.4 and pH 6.0, respectively. Blue fluorescence stained with Hoechst indicates cell nuclei; green fluorescence indicates MnAs@SiO_2-pHLIP.

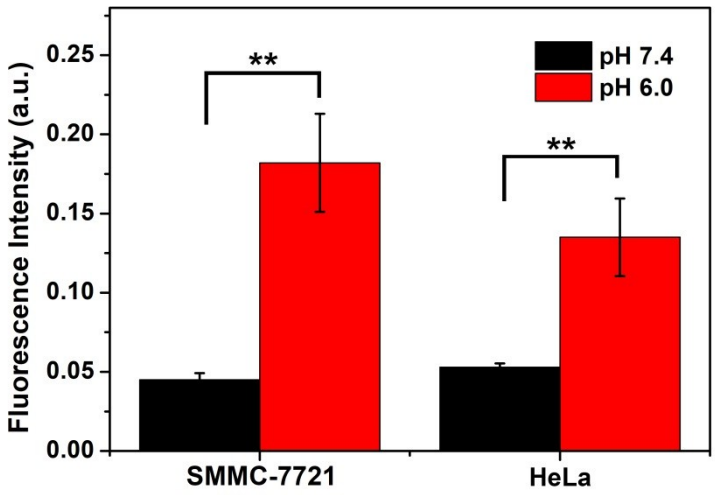

Figure S7. Semi-quantitative analysis of the fluorescence intensity of SMMC-7721 and HeLa cells incubated with MnAs@SiO_2-pHLIP in cell culture media of different pH values, corresponding to Figure 3d and Figure S6. Data are shown as mean ± SD, n = 4. Statistical analysis was performed with two-tailed Student's t-test, $^{**}p < 0.01$.

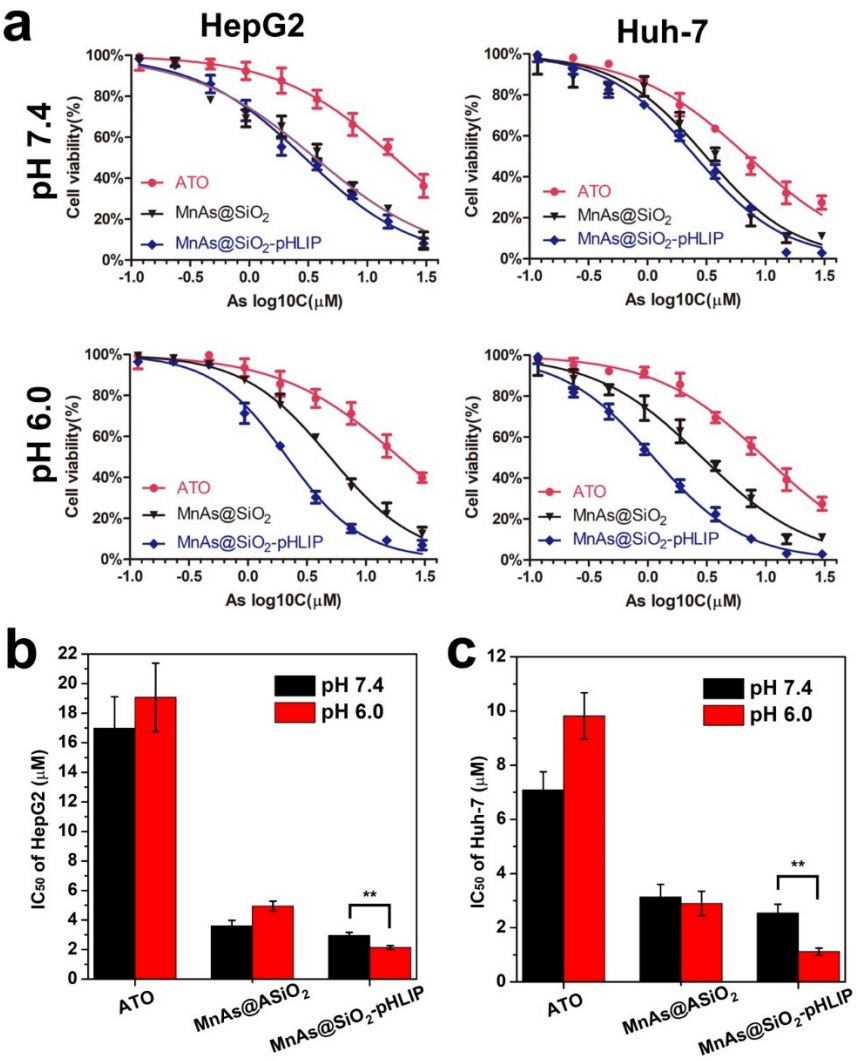

Figure S8. (a) Cell viabilities of HepG2 and Huh-7 cancer cells treated with ATO, MnAs@SiO_2, or MnAs@SiO_2-pHLIP for 48 h. Values are mean ± SD (n = 6). Comparison of IC_{50} values of ATO, MnAs@SiO_2, and MnAs@SiO_2-pHLIP against HepG2 (b) and Huh-7 (c) cancer cells for 48 h. Data are shown as mean ± SD; statistical analysis was performed with two-tailed Student's t-test; $^{**}p < 0.01$.

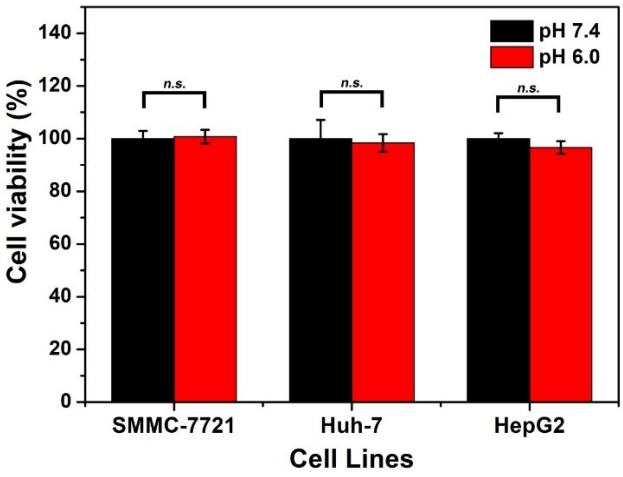

Figure S9. Cell viabilities of SMMC-7721, Huh-7, and HepG2 cells in cell culture media of pH 7.4 and pH 6.0. Data are shown as mean ± SD, $n = 4$. Statistical analysis was performed with two-tailed Student's *t*-test, *n.s*. represents not significant.

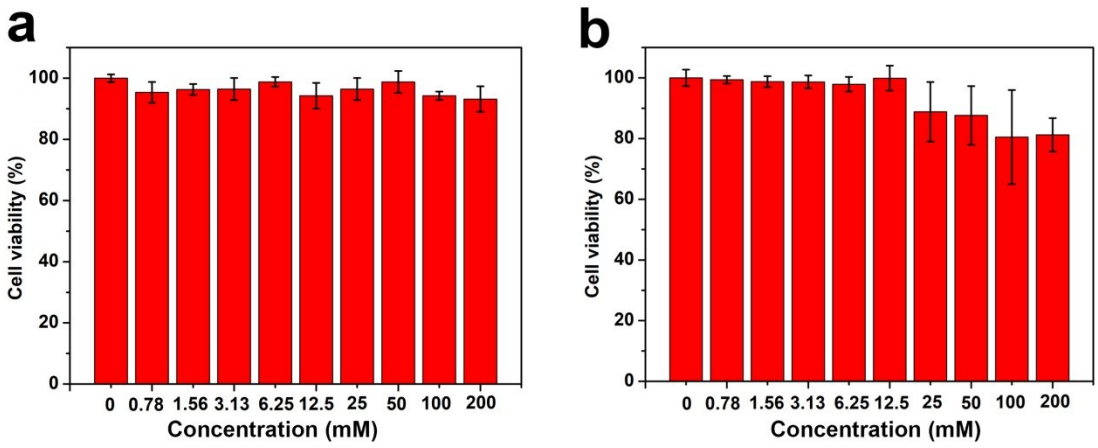

Figure S10. Cell viabilities of SMMC-7721 cells incubated with pHLIP (a) and $MnCl_2$ (b) for 48 h. The experiment was conducted at pH = 7.4. Data are shown as mean ± SD.

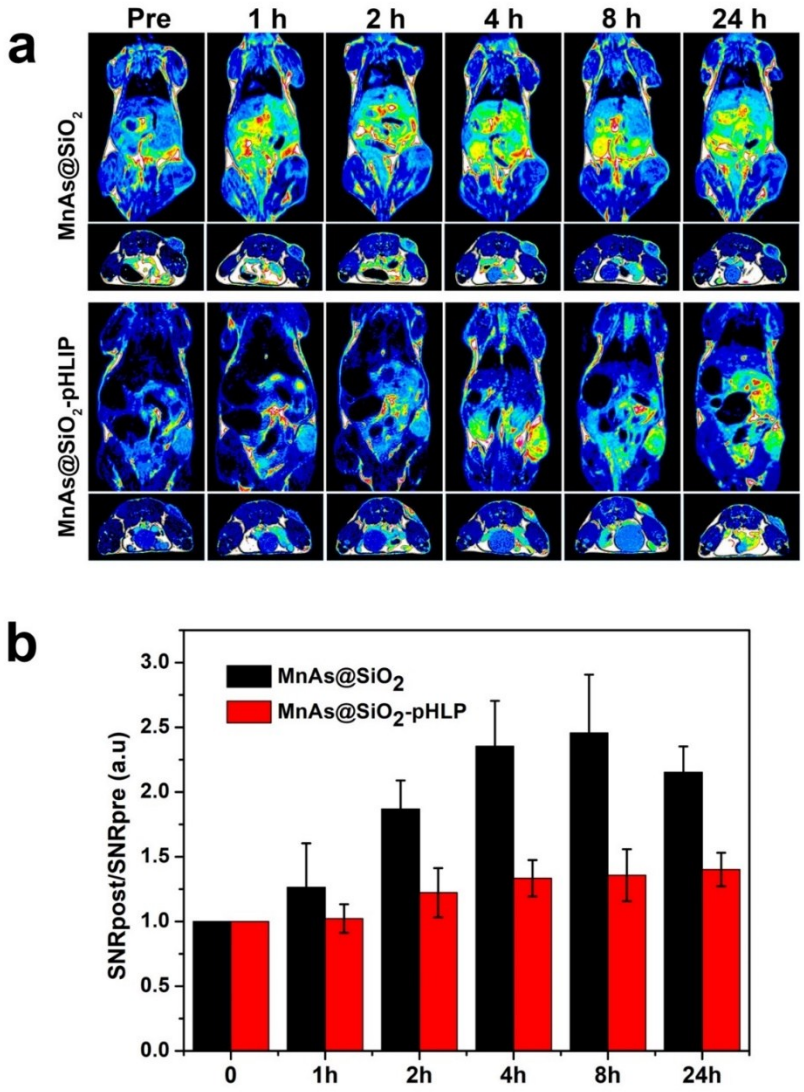

Figure S11. (a) Pseudocolor T_1-weighted MR images of mice intravenously injected with MnAs@SiO_2 or MnAs@SiO_2-pHLIP in the coronal plane and transverse plane at different time points. (b) Relative SNR_{liver}'s at different time points after treatment.

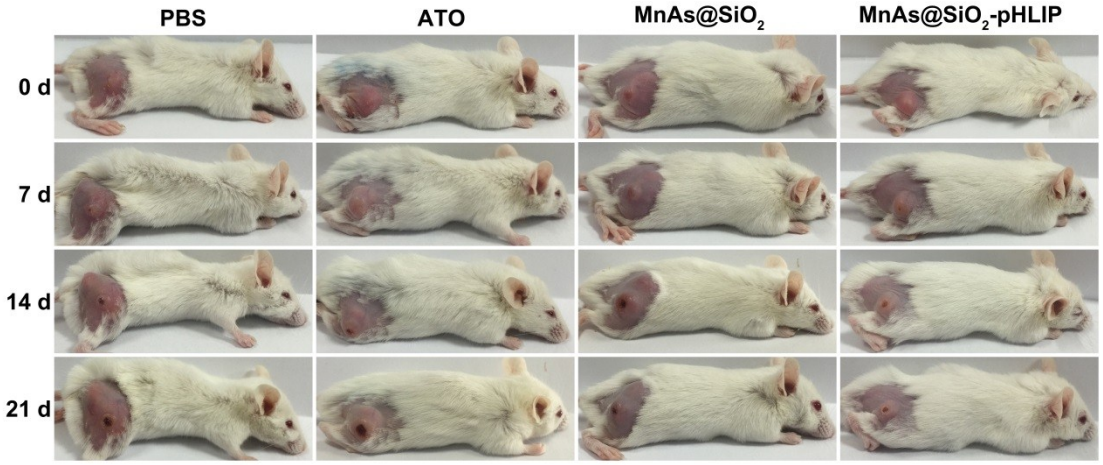

Figure S12. Optical images of mice from different treatment groups taken every 7 days.

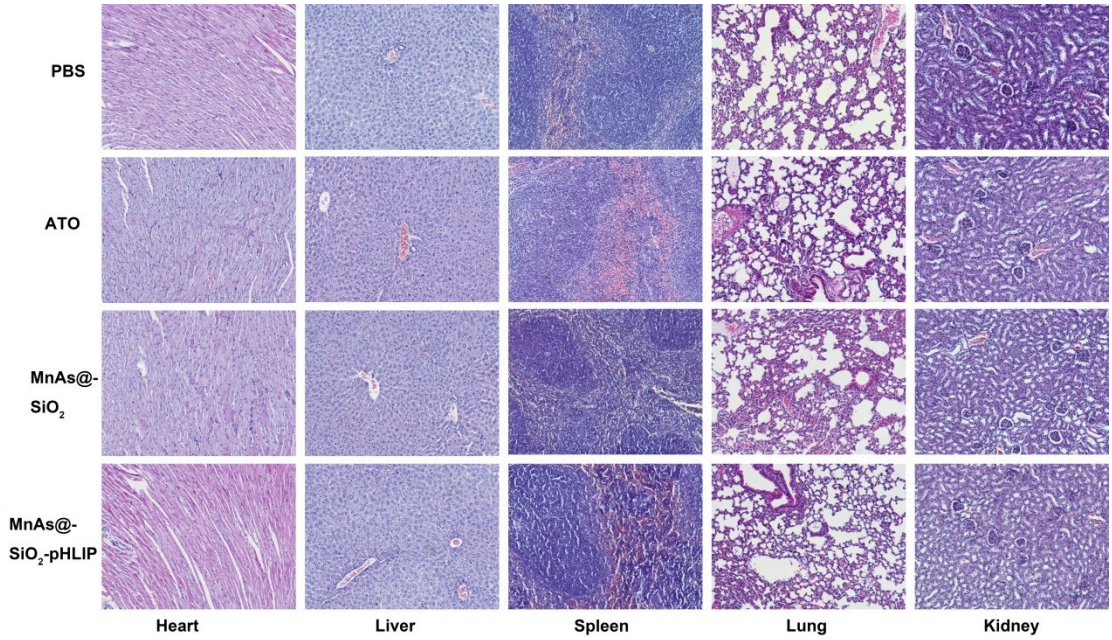

Figure S13. H&E stained images of major organs collected from mice at 4 weeks after various treatments.

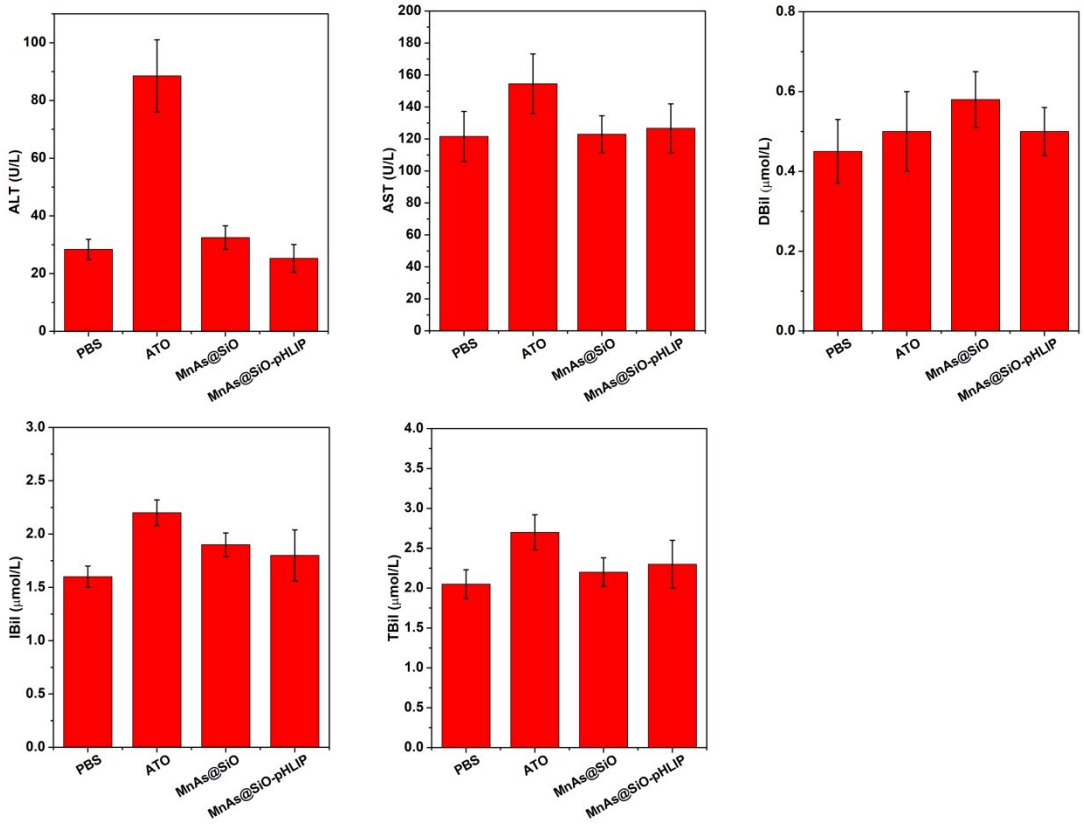

Figure S14. Blood biochemical indexes of mice treated with various formulations for 28 days.

Table S1. IC_{50} of ATO, MnAs@SiO_2, and MnAs@SiO_2-pHLIP against various cancer cells after 48 h incubation.

Cell	Tissue	ATO (μM)		MnAs@SiO_2 (μM)		MnAs@SiO_2-pHLIP(μM)	
		pH 7.4	pH 6.0	pH 7.4	pH 6.0	pH 7.4	pH 6.0
SMMC-7721	Human liver cancer	12.36±1.36	13.15±1.40	4.10±0.42	4.49±0.45	3.82±0.37	1.58±0.11
HepG2	Human liver cancer	16.97±2.14	19.07±2.31	3.60±0.381	4.95±0.33	2.95±0.22	2.14±0.13
Huh-7	Human liver cancer	7.21±1.51	9.54±1.26	3.22±0.68	2.98±0.55	2.40±0.23	1.22±0.08
A549	Human non-small cell lung cancer	8.04±1.26	8.65±1.56	3.65±0.512	4.03±0.42	3.02±0.33	1.62±0.22
HeLa	Human cervical cancer	7.83±0.85	9.28±0.99	3.13±0.49	2.89±0.46	2.45±0.22	1.12±0.05
H22	Mouse liver cancer	9.03±2.56	9.98±2.35	4.03±1.12	3.65±0.86	3.11±0.33	2.02±0.25

Notes:

1. IC_{50} is the half maximal inhibitory concentration.
2. Calculation of IC_{50} values is based on the concentration of arsenic.
3. Values are mean ± SD of three independent experiments.

Table S2. Quantitative analysis of the flow cytometry results of Figure 3e.

	Robust CV (FITC-A)	Geometric Mean (FITC-A)	Mean (FITC-A)
Control	221	247	271
$MnAs@SiO_2$ pH 7.4	595	950	4304
$MnAs@SiO_2$-pHLIP pH 7.4	634	959	3314
$MnAs@SiO_2$ pH 6.0	655	669	2190
$MnAs@SiO_2$-pHLIP pH 6.0	123	12675	20515